THE ASTROPHYSICAL JOURNAL, 389:179–187, 1992 April 10

EXOSAT OBSERVATIONS OF THE BROAD-LINE RADIO GALAXY 3C 382

K. K. GHOSH AND S. SOUNDARARAJAPERUMAL
Indian Institute of Astrophysics, Vainu Bappu Observatory, Kavalur, Alangayam, N.A., T.N., 635701 India
Received 1991 May 31; accepted 1991 October 17

ABSTRACT

X-ray observations of the broad-line radio galaxy 3C 382 were carried out with *EXOSAT* on many occasions (>20) between 1983 and 1985. Low and Medium Energy (LE and ME) spectra of this source were obtained from the *EXOSAT* data base. The hard X-ray luminosity light curve of 3C 382 which was constituted from *Ariel V*, *HEAO 1*, *Einstein*, *EXOSAT*, and *Ginga* observations between 1975 and 1989, shows a major outburst of this galaxy in 1985 during *EXOSAT* observations. During the outburst, both the LE and ME count rates displayed dramatic variations (maximum to minimum variations were ~120% and ~110% in the LE and ME bands, respectively, with different rise/decay time scales). Also, both the LE and ME light curves contain a prominent dip about halfway through. Although the variability of the LE and ME count rates was correlated, but the ME spectral slope was roughly constant ($\sim 1.7 \pm 0.1$) and the LE spectral slope varied in correlation with the LE count rate, with the soft excess and with the softness ratio of the source. Correlated variability was also observed between the LE count rate and the softness ratio of 3C 382 during the outburst. Spectra of this galaxy show the presence of an emission line at 6.2 ± 0.6 keV which may be due to fluorescence of cold iron around the central continuum source. The equivalent width of this line, which ranges between 100 and 1100 eV, did not vary during *EXOSAT* observations. The significance of these results is discussed.

Subject headings: galaxies: individual (3C 382) — galaxies: Seyfert — radiation mechanisms: bremsstrahlung — X-rays: galaxies

1. INTRODUCTION

Optical and ultraviolet observations of 3C 382 ($V = 15.39$; $M_V = -22.4$) displayed the presence of narrow and very broad variable emission lines (Osterbrock et al. 1975, 1976; Tadhunter, Perez, & Fosbury 1986; Yee & Oke 1978, 1981; Reichert et al. 1985). Ultraviolet (Osterbrock et al. 1976; Yee & Oke 1978) and infrared excesses (O'Dell et al. 1978; Puschell 1981) are present in the continuum energy distribution of this galaxy. It is a strong radio source with double radio lobes (MacDonald, Kenderdine, & Neville 1968; Riley & Branson 1973; Burch 1979; Parma et al. 1986; Preuss & Fosbury 1983; Storm, Willis, & Wilson 1978). Prior to *EXOSAT*, 3C 382 was observed with *Ariel V* (Elvis et al. 1978), *HEAO 1* A-2 (Marshall et al. 1979), *HEAO 1* MC (Dower et al. 1980), and *Einstein* (Petre et al. 1984; Urry et al. 1989) X-ray satellites. This radio-loud galaxy was also observed with *EXOSAT* on many occasions between 1983 and 1985, and recently it was observed with *Ginga* in 1989 July (Kastra, Kunieda, & Awaki 1991). The hard X-ray light curve of 3C 382 (see Fig. 5 of Kastra et al. 1991) shows a major outburst of this galaxy in 1985 during *EXOSAT* observations. Dramatic variations of both the low- and high-energy X-ray fluxes were found in 3C 382 during its flare. A doubling time of the X-ray flux of 3 days was detected from *EXOSAT* observations for this galaxy (Barr & Mushotzky 1986). In this paper we present the results of the spectral analysis of a large amount of *EXOSAT* data which has never been published before.

2. OBSERVATIONS, SPECTRAL ANALYSIS, AND RESULTS

EXOSAT observations of 3C 382 were carried out on many (>20) epochs between 1983 and 1985. Low (LE) and Medium Energy (ME) detectors which were sensitive in the 0.1–2 keV and 2–10 keV range, respectively, were used during the *EXOSAT* observations. A log of observations of 3C 382 is given in Table 1 with LE and ME count rates. In the present analysis we have used 13 good-quality spectra, when all the ME detectors were on, and we have excluded the spectra which have shorter exposures and poor signal-to-noise ratio. White & Peacock (1988) have described the *EXOSAT* instrumentation in detail. Details of the LE and ME detectors have been described by de Korte et al. (1981) and Turner, Smith, & Zimmermann (1981), respectively. LE data were obtained by using Lexan 3000 (LX3), aluminum/Parylene (Al/P) and boron (B) filters, ME data were collected from the eight argon-filled proportional counters (detectors) which were divided into two halves (detectors 1–4 and 5–8 are called half 1 and half 2, respectively). These two halves can be either aligned to the pointing axis or offset by 2° to monitor the background. Background-subtracted LE and ME spectra of 3C 382 were obtained from the *EXOSAT* data base. Observed LE and ME count rates are plotted in Figure 1. This figure shows the dramatic variations of the LE and ME count rates of this galaxy during its major outburst (see Fig. 5 of Kastra et al. 1991). In the next section, we will discuss in detail these remarkable variations of the LE and ME light curves.

Spectral analysis of the ME and LE + ME spectra were carried out using the XSPEC (X-ray Spectral Fitting) software package. ME spectra were fitted using a power law + absorption model (the interstellar absorption cross sections were obtained from Morrison & McCammon 1983), and the results of the spectral fits are given in Table 2A (model 1). Errors denote 90% errors for one interesting parameter which were computed following the procedure given by Lampton, Margon, & Bower (1976) ($\chi^2_{\rm min} + 4.61$ for two free parameters). Since model 1 yields a low hydrogen column density ($N_{\rm H}$), we

TABLE 1

LOG OF OBSERVATION OF THE LE AND ME SPECTRA AND COUNT RATES OF 3C 382

Start Time[a]	End Time[b]	LE Count Rate (LX3) (10^{-4} cm^{-2} s^{-1})	ME Count Rate[c] (10^{-3} cm^{-2} s^{-1})
1983, 255, 03:16	255, 09:10	3.76 ± 0.21	2.73 ± 0.06
1984, 130, 19:24	130, 22:58	8.07 ± 0.60	4.85 ± 0.14
1985, 109, 07:20	109, 11:03	4.09 ± 0.31	2.57 ± 0.10
1985, 109, 23:28	110, 03:11	4.09 ± 0.31	2.51 ± 0.09
1985, 116, 17:50	117, 00:18	4.13 ± 0.40	2.36 ± 0.11
1985, 117, 16:27	117, 21:29	4.13 ± 0.40	2.25 ± 0.06
1985, 147, 01:46	147, 05:10	5.05 ± 0.46	3.31 ± 0.07
1985, 153, 13:10	153, 16:50	6.90 ± 0.58	4.12 ± 0.07
1985, 161, 05:50	161, 11:45	6.49 ± 0.55	3.61 ± 0.05
1985, 171, 21:05	172, 01:56	6.77 ± 0.39	4.28 ± 0.06
1985, 178, 05:40	178, 12:01	6.47 ± 0.42	3.97 ± 0.14
1985, 195, 05:01	195, 07:30	7.08 ± 0.40	4.38 ± 0.08
1985, 204, 21:26	204, 23:10	4.23 ± 0.36	3.28 ± 0.15
1985, 211, 21:29	212, 09:20	6.21 ± 0.39	3.44 ± 0.05
1985, 223, 16:00	223, 18:49	7.51 ± 0.52	3.67 ± 0.07
1985, 233, 10:36	233, 13:15	7.85 ± 0.50	4.81 ± 0.08
1985, 246, 19:36	247, 00:50	8.17 ± 0.49	4.52 ± 0.06
1985, 256, 13:12	256, 19:26	8.57 ± 0.50	4.13 ± 0.06
1985, 273, 03:44	273, 09:39	8.97 ± 0.52	4.69 ± 0.12

[a] Format: year, day, hour:minutes.
[b] Format: day, hour:minutes.
[c] ME count rates are for PHA channels 1–35 corresponding to the energy range of 1–10 keV with the best signal-to-noise ratio.

fix the column density to the Galactic N_H value (7.4×10^{20} cm^{-2}; Stark et al 1992). This value of N_H is also consistent with the fact that a high-luminosity Seyfert galaxy such as 3C 382 suffers little from internal absorption (Mushotzky 1984). However, absorption was detected in this galaxy from *Einstein* data (99% lower and upper limit values of N_H were 7 times smaller and larger than the Galactic N_H value, respectively; Kruper, Urry, & Canizares 1990). Fit parameters of model 2 are given in Table 2B. ME spectral indices are plotted in Figures 2 and 3 against the date of observations and the ME count rate, respectively. From Table 2B and Figures 2 and 3 it is evident that the hard spectral slope (Γ) of 3C 382 did not vary (with time or count rate) during the major outburst of this galaxy. Average value of Γ of 3C 382 is around 1.7 (see Figs. 2 and 3), and this value of Γ is steeper than that obtained from *Ginga* data ($\Gamma = 1.49 \pm 0.05$; Kastra et al. 1991).

Power-law models with free (model 3) and fixed (model 4) absorbing column density were used to fit the combined LE + ME spectra of 3C 382, and the results are presented in Tables 3A & 3B, respectively. The LE + ME spectrum of 3C 382 which was observed on 1985/246, is plotted in Figure 4 with the best-fit power-law model convolved through the detector response. The lower panel of this figure shows the residuals between the model and the spectrum. Figures 5*a*–5*c* plot the residuals of different dates, and these figures show the presence

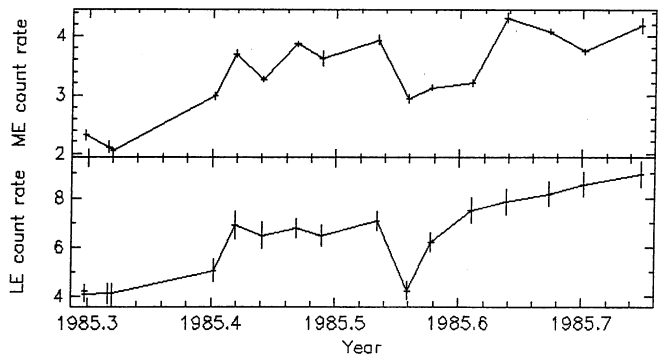

FIG. 1.—Plot of the LE and ME count rates vs. the date of observations. Note the remarkable dip in both the light curves about halfway through.

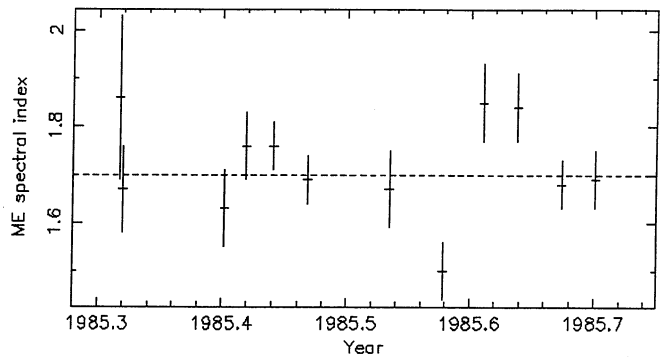

FIG. 2.—ME spectral index plotted against the date of observations. Dashed line shows the average value of the spectral index.

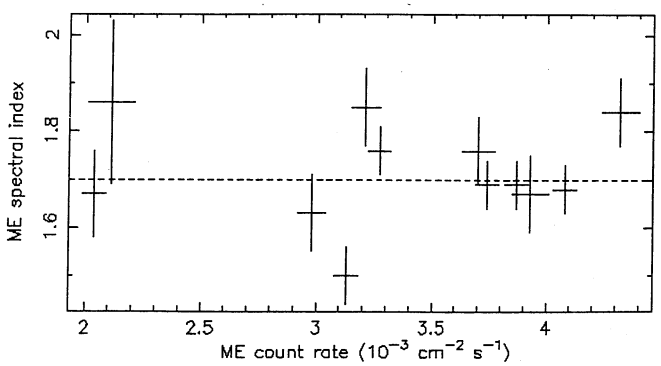

FIG. 3.—Same as Fig. 2 but for ME count rate

TABLE 2A

MODEL 1: POWER LAW + ABSORPTION FITS TO THE ME SPECTRA

Date (year/day)	Γ[a]	N[b]	N_H[c]	χ_r^2[d]
1983/255	$1.64^{+0.10}_{-0.09}$	$6.15^{+1.03}_{-0.65}$	$0 < 22$	0.80
1985/116	1.83	7.45	8.50	0.94
1985/117	$1.95^{+0.24}_{-0.23}$	$9.41^{+4.58}_{-2.92}$	91^{+68}_{-61}	1.81
1985/147	$1.71^{+0.20}_{-0.17}$	$8.79^{+3.38}_{-2.00}$	$0 < 82$	0.99
1985/153	$1.73^{+0.06}_{-0.07}$	$10.77^{+3.04}_{-0.92}$	$0 < 38$	0.96
1985/161	$1.88^{+0.13}_{-0.13}$	$12.22^{+2.89}_{-2.25}$	$0 < 70$	1.32
1985/171	$1.66^{+0.09}_{-0.06}$	$10.09^{+1.50}_{-0.71}$	$0 < 20$	0.87
1985/195	$1.64^{+0.09}_{-0.08}$	$9.91^{+1.70}_{-0.98}$	$0 < 22$	1.33
1985/211	$1.48^{+0.06}_{-0.07}$	$6.30^{+0.65}_{-0.50}$	$0 < 12$	0.98
1985/223	$1.83^{+0.15}_{-0.08}$	$10.68^{+2.88}_{-0.96}$	$0 < 35$	1.19
1985/233	$1.84^{+1.60}_{-1.00}$	$14.79^{+4.65}_{-1.93}$	$0 < 49$	1.21
1985/246	$1.65^{+0.06}_{-0.05}$	$10.58^{+0.96}_{-0.67}$	$0 < 12$	0.93
1985/256	$1.67^{+0.08}_{-0.06}$	$9.85^{+1.38}_{-0.69}$	$0 < 19$	0.62

[a] Photon index.
[b] Normalization in 10^{-3} photons cm^{-2} s^{-1} keV^{-1} at 1 keV.
[c] Column density in 10^{20} cm^{-2}.
[d] For 32 degrees of freedom.

TABLE 2B

MODEL 2: POWER LAW + FIXED ABSORPTION[a] FITS TO THE ME SPECTRA

Date (year/day)	Γ[b]	N[c]	χ_r^2[d]
1983/255	$1.66^{+0.09}_{-0.08}$	$6.42^{+0.74}_{-0.68}$	0.81
1985/116	$1.86^{+0.17}_{-0.17}$	$7.72^{+1.76}_{-1.48}$	0.95
1985/117	$1.67^{+0.09}_{-0.10}$	$5.83^{+0.73}_{-0.67}$	1.92
1985/147	$1.63^{+0.08}_{-0.08}$	$7.76^{+0.88}_{-0.81}$	0.99
1985/153	$1.76^{+0.07}_{-0.07}$	$11.28^{+1.05}_{-0.98}$	0.96
1985/161	$1.76^{+0.06}_{-0.05}$	$10.16^{+0.72}_{-0.68}$	1.36
1985/171	$1.69^{+0.05}_{-0.06}$	$10.56^{+0.79}_{-0.76}$	0.87
1985/195	$1.67^{+0.08}_{-0.08}$	$10.37^{+1.12}_{-1.03}$	1.34
1985/211	$1.50^{+0.07}_{-0.06}$	$6.58^{+0.58}_{-0.55}$	1.00
1985/223	$1.85^{+0.08}_{-0.08}$	$11.19^{+1.10}_{-1.02}$	1.19
1985/233	$1.84^{+0.07}_{-0.07}$	$14.71^{+1.35}_{-1.27}$	1.22
1985/246	$1.68^{+0.05}_{-0.06}$	$11.06^{+0.73}_{-0.70}$	0.95
1985/256	$1.69^{+0.06}_{-0.05}$	$10.31^{+0.76}_{-0.73}$	0.63

[a] Fixed at the Galactic N_H value (7.4×10^{20} cm^{-2}).
[b] Photon index.
[c] Normalization in 10^{-3} photons cm^{-2} s^{-1} keV^{-1} at 1 keV.
[d] For 33 degrees of freedom.

of soft excess in 3C 382. Soft excess values measured from the residuals are given in Table 4. LE count rate versus soft excess is plotted in Figure 6. It is evident from this figure that the soft excess was variable and the variability was correlated with the variations of the LE count rate (coefficient of the linear regression fit is 0.89 for 12 observations which means that the probability of the fit being random is ~0.05%). Also Figure 7 shows that the soft excess is correlated with the softness ratio (LE count rate/ME count rate) of the source (correlation coefficient is 0.77 for 13 observations).

Fit parameters of model 3 (see Table 3A) show that the values of N_H, for all the spectra, are smaller than the Galactic N_H value. "Negative N_H" values imply a source spectrum with more emission than the power-law prediction at low energies,

TABLE 3A

MODEL 3: POWER LAW + ABSORPTION FITS TO THE LE + ME SPECTRA

Date (year/day)	Γ[a]	N[b]	N_H[c]	χ_r^2[d]
1983/255	$1.65^{+0.09}_{-0.09}$	$6.28^{+0.78}_{-0.69}$	$4.1^{+1.40}_{-1.10}$	0.79
1985/116	$1.85^{+0.18}_{-0.18}$	$7.65^{+1.93}_{-1.55}$	$5.68^{+3.61}_{-2.35}$	0.90
1985/117	$1.66^{+0.09}_{-0.10}$	$5.70^{+0.75}_{-0.07}$	$3.11^{+1.48}_{-1.00}$	1.93
1985/147	$1.62^{+0.08}_{-0.08}$	$7.59^{+0.90}_{-0.08}$	$3.40^{+1.51}_{-1.02}$	0.98
1985/153	$1.75^{+0.07}_{-0.07}$	$11.05^{+1.10}_{-1.00}$	$4.23^{+1.49}_{-1.07}$	0.94
1985/161	$1.76^{+0.06}_{-0.06}$	$9.97^{+0.75}_{-0.70}$	$4.04^{+1.29}_{-0.92}$	1.37
1985/171	$1.67^{+0.06}_{-0.06}$	$10.31^{+0.83}_{-0.76}$	$3.66^{+0.95}_{-0.75}$	0.85
1985/195	$1.66^{+0.08}_{-0.09}$	$10.09^{+1.15}_{-1.03}$	$3.25^{+1.07}_{-0.83}$	1.30
1985/211	$1.48^{+0.07}_{-0.06}$	$6.35^{+0.58}_{-0.54}$	$1.54^{+0.53}_{-0.32}$	0.96
1985/223	$1.84^{+0.08}_{-0.08}$	$10.95^{+1.14}_{-1.04}$	$4.02^{+1.23}_{-0.94}$	1.15
1985/233	$1.83^{+0.08}_{-0.07}$	$14.54^{+1.46}_{-1.32}$	$5.60^{+1.60}_{-1.24}$	1.17
1985/246	$1.66^{+0.05}_{-0.05}$	$10.75^{+0.75}_{-0.70}$	$2.89^{+0.71}_{-0.57}$	0.92
1985/256	$1.67^{+0.06}_{-0.05}$	$9.99^{+0.78}_{-0.72}$	$2.46^{+0.63}_{-0.51}$	0.60

[a] Photon index.
[b] Normalization in 10^{-3} photons cm^{-2} s^{-1} keV^{-1} at 1 keV.
[c] Column density in 10^{20} cm^{-2}.
[d] For 33 degrees of freedom.

i.e., a "soft excess" (Wilkes & Elvis 1987; Kruper et al. 1990). Also it can be seen from the contour plots in Wilkes & Elvis (1987) that forcing a column density in the presence of a soft excess always steepens the spectral slope. This type of spectral steepening is also present in 3C 382 which can be seen from the comparison of the Γ values between Tables 3A and 3B. In such a situation, it is better to make a two-component fit to the LE + ME data. Two power law (model 5), thermal bremsstrahlung (model 6), and broken power-law (model 7) models were used to fit to the LE + ME spectra of 3C 382. Since the average value of the ME spectral index of this galaxy is $\sim 1.7 \pm 0.10$ (see Figs. 2 and 3), we have therefore fixed the value of the hard component slope (for two-component fits) with 1.7. Best-fit parameters of models 5–7 are given in Tables

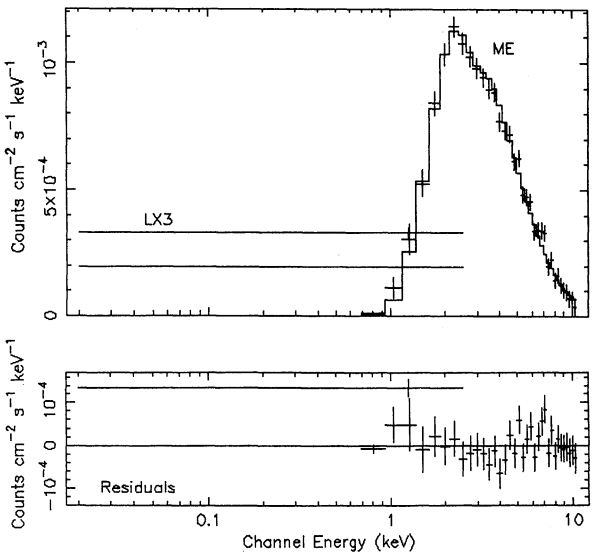

FIG. 4.—Observed LE + ME spectrum of 3C 382 fitted with a simple power law and fixed absorption model. Lower panel of the figure shows the residual between the spectrum and the model.

TABLE 3B

MODEL 4: POWER LAW + FIXED ABSORPTION[a] FITS TO THE LE + ME SPECTRA

DATE (year/day)	Γ[b]	N[c]	FLUX[d] 0.1–2 (keV)	FLUX[d] 2–10 (keV)	L_X[e] 0.1–2 (keV)	L_X[e] 2–10 (keV)	χ_r^2[f]
1983/255	$1.80^{+0.05}_{-0.06}$	$7.65^{+0.51}_{-0.61}$	1.41 ± 0.08	2.77 ± 0.06	2.14 ± 0.12	4.21 ± 0.09	1.10
1985/116	$1.93^{+0.09}_{-0.10}$	$8.50^{+0.90}_{-0.93}$	1.35 ± 0.13	2.66 ± 0.12	2.05 ± 0.19	4.04 ± 0.18	0.92
1985/117	1.78	6.75	1.25 ± 0.12	2.48 ± 0.07	1.90 ± 0.18	3.77 ± 0.11	2.25
1985/147	$1.73^{+0.07}_{-0.07}$	$8.80^{+0.80}_{-0.80}$	1.74 ± 0.16	3.44 ± 0.07	2.64 ± 0.24	5.23 ± 0.11	1.30
1985/153	$1.83^{+0.06}_{-0.06}$	$12.33^{+0.96}_{-0.93}$	2.16 ± 0.18	4.26 ± 0.07	3.28 ± 0.27	6.48 ± 0.11	1.18
1985/161	$1.82^{+0.05}_{-0.06}$	$10.82^{+0.70}_{-0.68}$	1.93 ± 0.16	3.80 ± 0.05	2.93 ± 0.24	5.78 ± 0.08	1.67
1985/171	$1.79^{+0.05}_{-0.05}$	$12.03^{+0.73}_{-0.72}$	2.22 ± 0.13	4.38 ± 0.06	3.38 ± 0.20	6.66 ± 0.09	1.54
1985/195	$1.85^{+0.06}_{-0.06}$	$13.01^{+0.89}_{-0.90}$	2.24 ± 0.13	4.43 ± 0.08	3.41 ± 0.20	6.73 ± 0.12	1.96
1985/211	1.66	8.07	1.75 ± 0.11	3.45 ± 0.05	2.66 ± 0.17	5.25 ± 0.08	3.00
1985/223	$1.96^{+0.07}_{-0.06}$	$12.90^{+0.93}_{-0.94}$	1.93 ± 0.13	3.80 ± 0.07	2.94 ± 0.20	5.78 ± 0.11	1.54
1985/233	$1.89^{+0.06}_{-0.05}$	$15.78^{+0.99}_{-0.98}$	2.57 ± 0.16	5.08 ± 0.09	3.91 ± 0.24	7.73 ± 0.14	1.25
1985/246	1.77	12.54	2.35 ± 0.14	4.65 ± 0.06	3.57 ± 0.21	7.07 ± 0.09	2.16
1985/256	1.82	12.22	2.16 ± 0.13	4.26 ± 0.06	3.29 ± 0.19	6.48 ± 0.09	2.23

[a] Fixed at the Galactic N_H value (7.4×10^{20} cm^{-2}).
[b] Photon index.
[c] Normalization in 10^{-3} photons cm^{-2} s^{-1} keV^{-1} at 1 keV.
[d] Flux in 10^{-11} ergs cm^{-2} s^{-1}.
[e] Luminosity in 10^{44} ergs s^{-1}.
[f] For 34 degrees of freedom.

3C–3E, respectively. A two power law model fits well to the data, but this model is insensitive to compute the error bars of the fit parameters. A thermal bremsstrahlung model is not acceptable because the χ_r^2 values are greater than 2.0. However, runs made with the broken power law model (break energy fixed at 0.6 keV, following Wilkes et al. 1989) resulted in a better fit. *F*-test results computed between this model (model 7) and the power-law model (model 4) show that the inclusion of the soft power-law (Γ_1) component is highly significant (>99.9%). Figure 8 shows the observed LE + ME spectrum fitted with the broken power law model convolved through the detector response. Residuals of the fit are shown in the lower part of this figure. Now, no soft excesses can be seen in the residuals of Figure 8. Soft spectral indices (obtained from the broken power law fits) versus the softness ratio of 3C 382 are plotted in Figure 9 which show that these two parameters are correlated (correlation coefficient is 0.93 for 13 observations which indicates that the fit is highly significant).

Recent results obtained from the *EXOSAT* and *Ginga* (Nandra et al. 1989; Leighly et al. 1989; Singh, Rao, & Vahia

TABLE 3C

MODEL 5: TWO POWER LAW[a] + FIXED ABSORPTION[b] FITS TO THE LE + ME SPECTRA

Date (year/day)	Γ_1[c]	N_1[d]	N_2[e]	χ_r^2[f]
1983/255	3.91	0.51	6.69	0.80
1985/116	2.41	3.39	4.93	0.90
1985/117	4.90	0.32	6.04	1.88
1985/147	5.51	0.19	7.69	0.95
1985/153	3.59	1.69	10.60	0.91
1985/161	$3.41^{+6.59}_{-0.72}$	$2.19^{+1.51}_{-2.19}$	$9.02^{+0.40}_{-0.74}$	1.38
1985/171	2.71	5.62	6.99	0.80
1985/195	$4.76^{+5.24}_{-1.68}$	$0.60^{+2.37}_{-0.50}$	$10.70^{+0.31}_{-0.62}$	1.29
1985/211	5.71	0.26	7.44	1.16
1985/223	$2.94^{+0.56}_{-0.42}$	$4.85^{+2.04}_{-1.90}$	$8.10^{+0.80}_{-1.36}$	1.15
1985/233	$2.28^{+0.36}_{-0.37}$	$8.95^{+6.21}_{-2.73}$	$7.00^{+2.07}_{-6.32}$	1.16
1985/246	$2.72^{+1.37}_{-0.45}$	$8.04^{+5.25}_{-6.31}$	$6.17^{+4.50}_{-4.42}$	0.80
1985/256	$4.73^{+5.27}_{-1.13}$	$1.02^{+2.02}_{-0.72}$	$10.35^{+0.23}_{-0.37}$	0.60

[a] Γ_2 fixed with 1.7.
[b] Fixed at the Galactic N_H value (7.4×10^{20} cm^{-2}).
[c] Photon index.
[d] Normalization in 10^{-3} photons cm^{-2} s^{-1} keV^{-1} at 1 keV.
[e] For 34 degrees of freedom.

TABLE 3D

MODEL 6: THERMAL BREMSSTRAHLUNG + FIXED ABSORPTION[a] FITS TO THE LE + ME SPECTRA

Date (year/day)	kT[b]	N[c]	χ_r^2[d]
1983/255	7.78	2.88	3.00
1985/116	$4.83^{+1.45}_{-0.95}$	$4.15^{+1.06}_{-0.89}$	1.40
1985/117	8.51	2.40	2.57
1985/147	$9.93^{+2.57}_{-1.77}$	$2.99^{+0.45}_{-0.41}$	1.90
1985/153	7.80	4.39	2.25
1985/161	7.89	3.89	2.52
1985/171	8.89	4.11	3.71
1985/195	7.77	4.58	4.38
1985/211	15.82	2.32	4.48
1985/223	6.03	4.84	3.32
1985/233	6.15	6.37	2.88
1985/246	9.67	4.11	4.49
1985/256	8.93	3.97	4.69

[a] Fixed at the Galactic N_H value (7.4×10^{20} cm^{-2}).
[b] Plasma temperature in keV.
[c] Normalization in 10^{-3} photons cm^{-2} s^{-1} keV^{-1} at 1 keV.
[d] For 34 degrees of freedom.

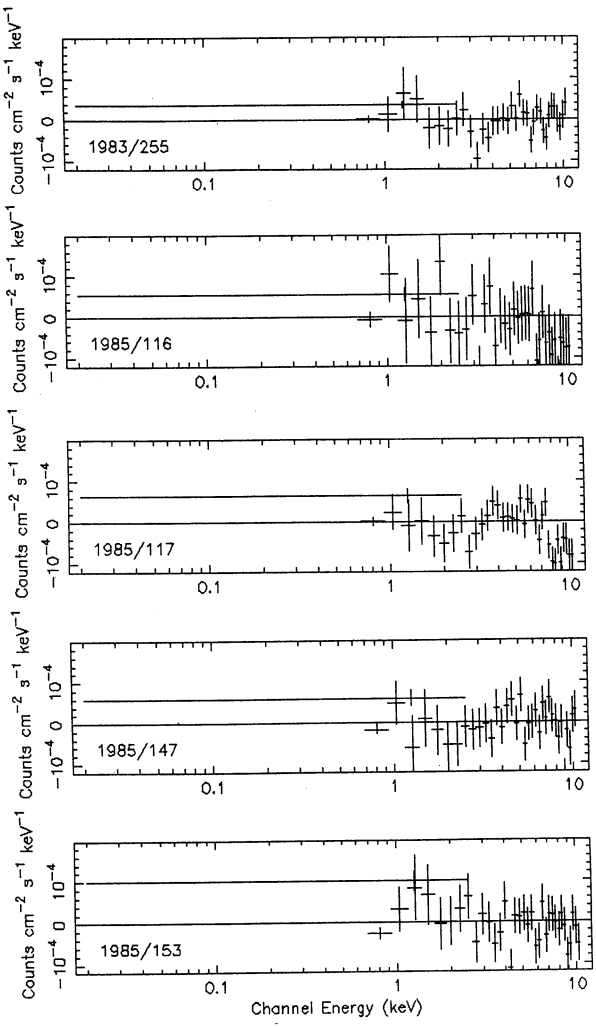

FIG. 5a

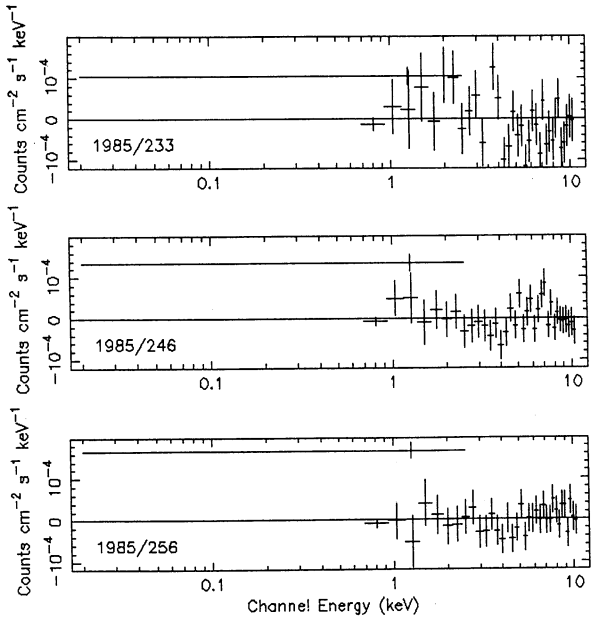

FIG. 5c

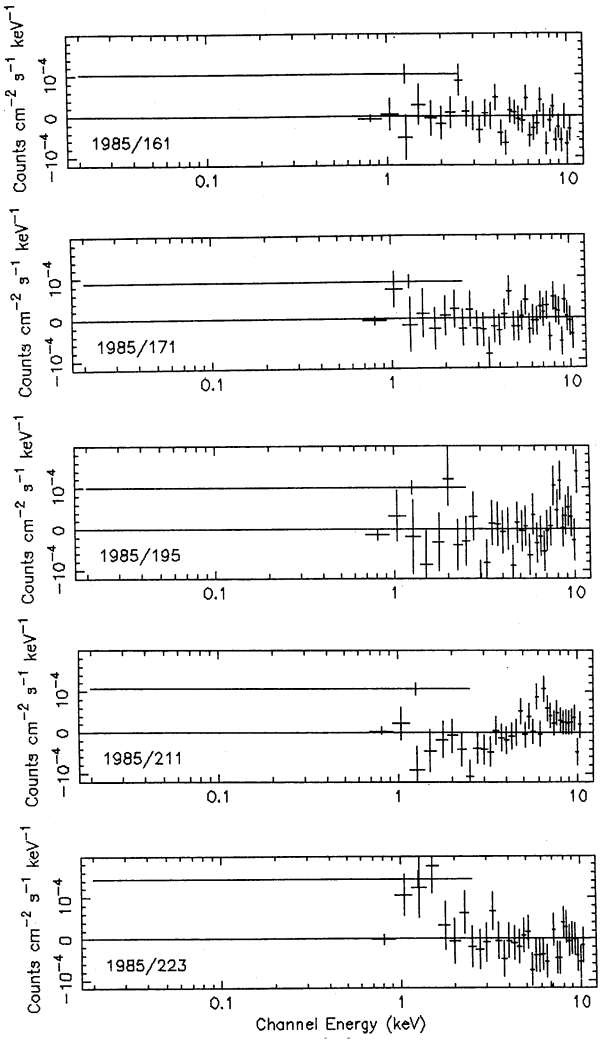

FIG. 5b

1990; Ghosh & Soundararajaperumal 1991; Pounds et al. 1989, 1990; Kastra et al. 1991) observations have provided strong evidences for the presence of Fe K-shell emission and absorption lines in the X-ray spectra of AGNs. Residuals of Figures 5*a*–5*c* also display the presence of an emission feature around 6.0 keV. Also an iron emission line has already been detected in the spectra of 3C 382, obtained from *Ginga* observations (Kastra et al. 1991). We have therefore added a Gaussian line feature (with a fixed line width of 0.1 keV and variable line center energy) with the power-law model (model 4) and were fitted to the 3C 382 data. Best-fit parameters of this model (model 8) are given in Table 3F. *F*-test computations between models 4 and 8 show that the inclusion of the Gaussian line is highly significant (>99.9%). Average line center energy is best estimated to be 6.2 ± 0.6 keV and the equivalent width of this line ranges between 100 and 1100 eV. Only statistical errors have been considered to estimate the range of values of the equivalent width. LE + ME spectrum with the best-fit Gaussian line model convolved through the detector response is

FIG. 5.—Residuals between the observed spectra and the model (power law + fixed absorption) are plotted for 13 observations. This figure clearly shows the presence of soft excess in 3C 382 which is also variable.

TABLE 3E

MODEL 7: BROKEN POWER LAW[a] + FIXED ABSORPTION[b] FITS TO THE LE + ME SPECTRA

Date (year/day)	Γ_1[c]	N[d]	χ_r^2[e]
1983/255	$3.04^{+0.33}_{-0.40}$	$3.88^{+0.33}_{-1.05}$	0.80
1985/116	$3.54^{+0.46}_{-0.63}$	$2.49^{+1.03}_{-0.58}$	0.95
1985/117	$3.71^{+0.39}_{-0.58}$	$2.17^{+0.76}_{-0.43}$	1.87
1985/147	$3.30^{+0.45}_{-0.63}$	$3.72^{+1.45}_{-0.79}$	1.05
1985/153	$3.61^{+0.38}_{-0.50}$	$3.94^{+1.17}_{-0.71}$	0.98
1985/161	$3.76^{+0.35}_{-0.48}$	$3.26^{+0.91}_{-0.56}$	1.45
1985/171	$3.46^{+0.29}_{-0.35}$	$4.35^{+0.87}_{-0.61}$	0.85
1985/195	$3.60^{+0.26}_{-0.33}$	$4.05^{+0.78}_{-0.56}$	1.29
1985/211	$3.92^{+0.27}_{-0.32}$	$2.70^{+0.50}_{-0.36}$	1.72
1985/223	$4.17^{+0.27}_{-0.33}$	$2.60^{+0.50}_{-0.36}$	1.46
1985/233	$3.47^{+0.31}_{-0.39}$	$5.00^{+1.14}_{-0.76}$	1.45
1985/246	$3.84^{+0.26}_{-0.30}$	$3.80^{+0.66}_{-0.48}$	0.94
1985/256	$4.21^{+0.23}_{-0.27}$	$2.87^{+0.44}_{-0.33}$	0.61

[a] Γ_2 fixed with 1.7. Break energy fixed at 0.6 keV.
[b] Fixed at the Galactic N_H value (7×10^{20} cm^{-2}).
[c] Photon index.
[d] Normalization in 10^{-3} photons cm^{-2} s^{-1} keV^{-1} at 1 keV.
[e] For 34 degrees of freedom.

shown in Figure 10. We also used the line absorption edge component with model 8 to fit to the data, but there were no improvements in χ^2 statistics than that obtained from model 8. We used the partial covering model to fit to the 3C 382 data, but it did not result in a better fit.

3. DISCUSSION

3.1. *Light Curve*

Hard (2–10 keV) X-ray luminosities of 3C 382 which were obtained from *Ariel V* (Elvis et al. 1978), *HEAO 1* (Marshall et al. 1979; Dower et al. 1980; Mushotzky 1984), *Einstein* (Petre et al. 1984; Urry et al. 1989), *EXOSAT* (see Table 3B), and *Ginga* (Kastra et al. 1991) data show that there was a strong outburst of this galaxy in 1985 during *EXOSAT* observations (see Fig. 5 of Kastra et al. 1991). Light curves of the LE and ME count rates during the outburst are plotted in Figure 1. This figure shows that 3C 382 displayed dramatic variations of the LE and ME count rates during the remarkable flare. The maximum variability range is ~120% for the LE energy band and ~110% for the ME energy band. These values of variabilities correspond to maximum to minimum count rates (rise/decay time scales are different for the LE and ME energy bands). Close inspection of Figure 1 shows that both the light curves contain a dip about halfway through, and the dip of the ME light curve is relatively broader than that of the LE. This is due to different rise time scales and amplitudes of variations of the LE and ME count rates. Figure 11, which plots the LE versus ME count rates, shows that the LE and ME variations are correlated (correlation coefficient is 0.90 for 17 observa-

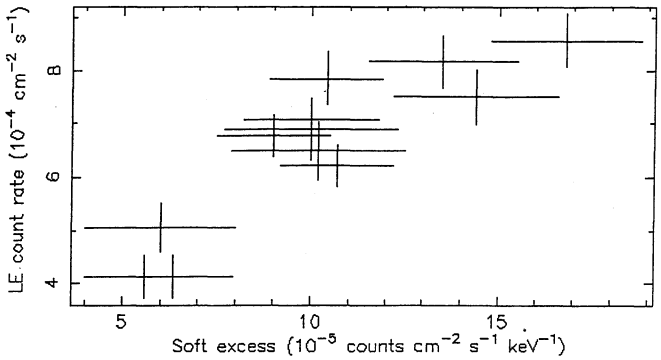

FIG. 6.—Plot of the soft excess vs. LE count rate. Correlated variability is evident between these two parameters.

TABLE 3F

MODEL 8: POWER LAW + FIXED ABSORPTION + GAUSSIAN LINE FITS TO THE LE + ME SPECTRA

Date (year/day)	Γ[b]	N[c]	E_L[d]	E_N[e]	EW[f]	χ_r^2[g]
1983/255	$1.85^{+0.06}_{-0.06}$	$7.92^{+0.52}_{-0.53}$	$5.45^{+0.39}_{-0.34}$	$1.28^{+0.63}_{-0.62}$	240 ± 120	0.81
1985/116	$1.98^{+0.09}_{-0.11}$	$8.64^{+0.86}_{-0.91}$	$5.62^{+0.40}_{-0.40}$	$1.32^{+0.62}_{-0.62}$	280 ± 125	0.86
1985/117	$1.88^{+0.06}_{-0.06}$	$7.28^{+0.50}_{-0.50}$	$5.62^{+1.07}_{-3.36}$	$1.38^{+1.21}_{-1.37}$	270 ± 255	1.87
1985/147	$1.77^{+0.08}_{-0.08}$	$9.14^{+0.86}_{-0.87}$	$7.06^{+0.62}_{-1.11}$	$1.18^{+1.10}_{-1.10}$	300 ± 280	1.20
1985/153	$1.86^{+0.07}_{-0.06}$	$12.67^{+1.02}_{-1.00}$	$7.13^{+14.9}_{-7.13}$	$1.08^{+1.12}_{-1.08}$	250 ± 250	1.11
1985/161	$1.86^{+0.06}_{-0.06}$	$11.20^{+0.78}_{-0.76}$	$5.51^{+0.85}_{-0.57}$	$0.76^{+0.64}_{-0.62}$	165 ± 135	1.60
1985/171	$1.82^{+0.05}_{-0.05}$	$12.41^{+0.77}_{-0.77}$	$7.26^{+1.28}_{-1.14}$	$1.36^{+1.01}_{-0.96}$	310 ± 225	1.43
1985/195	$1.87^{+0.06}_{-0.06}$	$13.23^{+1.10}_{-1.00}$	$5.32^{+0.50}_{-0.50}$	$0.79^{+0.62}_{-0.62}$	115 ± 90	1.84
1985/211	1.78	9.11	6.54	2.35	740 ± 410	2.43
1985/223	$2.03^{+0.07}_{-0.07}$	$13.36^{+0.98}_{-0.97}$	$4.58^{+0.44}_{-0.41}$	$1.35^{+0.80}_{-0.80}$	225 ± 130	1.34
1985/233	$1.91^{+0.06}_{-0.05}$	$15.87^{+1.01}_{-0.99}$	$4.07^{+1.44}_{-0.81}$	$0.76^{+1.01}_{-0.76}$	60 ± 60	1.12
1985/246	$1.84^{+0.06}_{-0.05}$	$13.41^{+0.84}_{-0.80}$	$6.76^{+0.42}_{-0.38}$	$2.16^{+0.82}_{-0.83}$	370 ± 140	1.71
1985/256	$1.89^{+0.07}_{-0.07}$	$12.96^{+0.90}_{-0.90}$	$6.57^{+0.40}_{-0.40}$	$1.63^{+0.75}_{-0.75}$	315 ± 145	1.82

[a] Fixed at the Galactic N_H value (7.4×10^{20} cm^{-2}).
[b] Photon index.
[c] Normalization in 10^{-3} photons cm^{-2} s^{-1} keV^{-1} at 1 keV.
[d] Line energy in keV.
[e] Line intensity in 10^{-4} photons cm^{-2} s^{-1}.
[f] Equivalent width in eV.
[g] For 32 degrees of freedom.

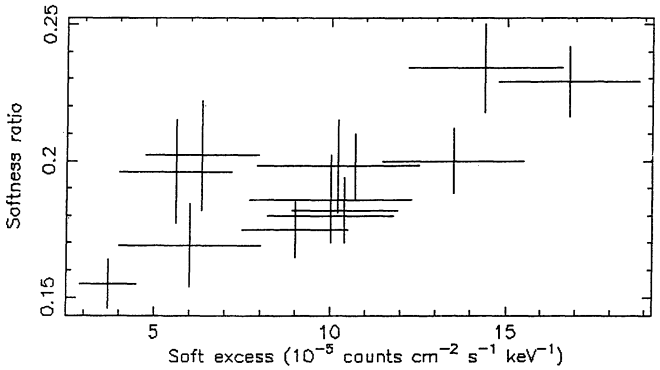

FIG. 7.—Same as Fig. 6 but for softness ratio of 3C 382

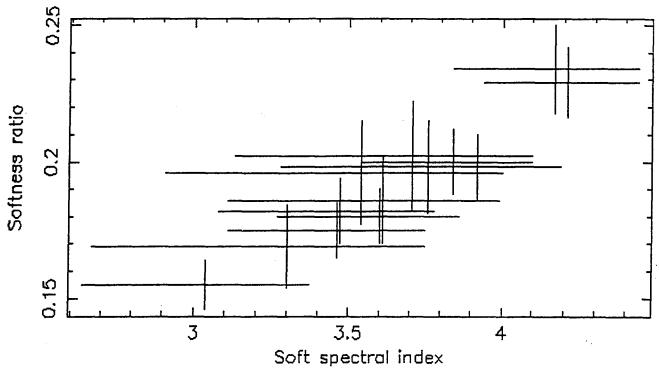

FIG. 9.—Soft spectral index is plotted against the softness ratio

tions which means that the probability of the fit being random is ~0.05%), but a few points lie on lower and upper lines. This type of variability between the low- and high-energy bands have also been observed in other Seyfert galaxies (Lawrence et al. 1985; Kunieda et al. 1990). However, no evidence for a correlation of the variability in the low- and high-energy bands was found in *Ginga* data for 3C 382 (Kastra et al. 1991) when this galaxy was ~4 times lower than during the *EXOSAT* observations. Correlated variability of the LE and ME count rates suggest that both the soft and hard X-rays, most probably, have a common origin. However, the plots of the LE and ME count rates against the softness ratio (Figs 12 and 13) show that the LE and ME count rates are correlated and uncorrelated with the softness ratio of the source, respectively. The softness-intensity effect seen in Figure 12 suggests the presence of a soft spectral effect (source softens as it brightens and vice versa) in 3C 382 which indicates a nonlinear relation between the LE and ME count rates (Lawrence et al. 1985). Also we have found the correlated variability between the soft spectral index and the softness ratio of the source (see Fig. 9), but no variations of the ME spectral index were seen with the ME count rate (see Figs. 2 and 3) or the softness ratio of the source during its flare. All these results suggest that the soft and hard X-rays originate from distinct sources. Most probably, the soft and hard X-rays originate in optically thin and thick parts of an accretion disk, respectively (Czerny & Elvis 1987).

3.2. *Soft Excess*

At present it is well accepted that soft excesses are common features of emission-line AGNs (references on individual AGNs may be obtained from Turner & Pounds 1989 and Kruper et al. 1990). Significant soft excess was detected in 3C 382 from *Einstein* IPC + MPC data, but *Einstein* SSS + MPC data displayed no evidence for soft excess in this galaxy (Urry et al. 1989). However, *EXOSAT* results show the presence of variable soft excess in this galaxy (see Figs 5*a*–5*c* and Table 4) which is correlated with the LE count rate (see Fig. 6), with the soft spectral slope (Γ_1) and with the softness ratio of the source (see Fig. 7). It is important to mention here that although the variability of the LE and ME count rates was correlated (see Fig. 11), but the ME spectral slope was roughly constant (average value was 1.7 ± 0.1). Also there is no evidence for correlation between the ME count rate and the softness ratio of the source (see Fig. 13). These results suggest that the soft

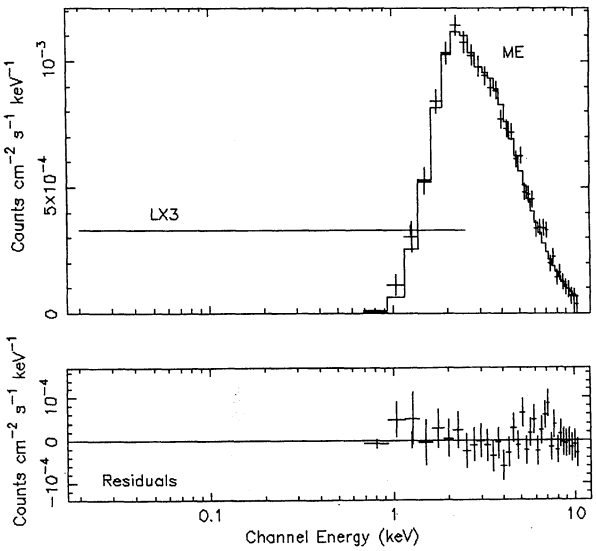

FIG. 8.—Observed spectrum of 3C 382 fitted with the broken power law model (model 7). Lower panel of the figure shows the residuals between the spectra and the model.

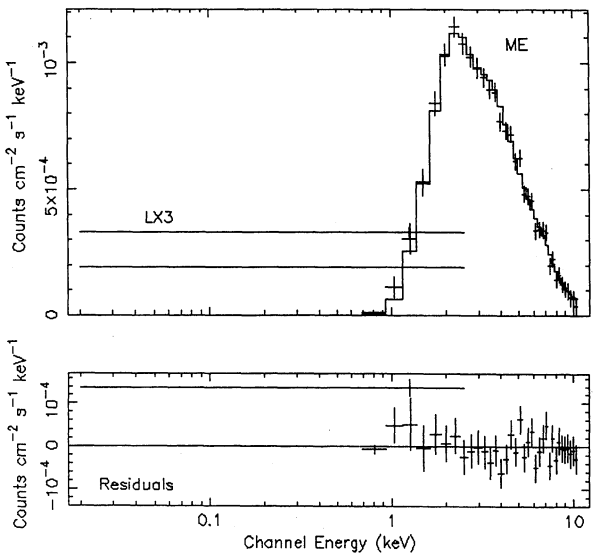

FIG. 10.—Observed spectrum of 3C 382 fitted with the Gaussian line model (model 8). Lower panel of the figure shows the residuals between the spectrum and the mode..

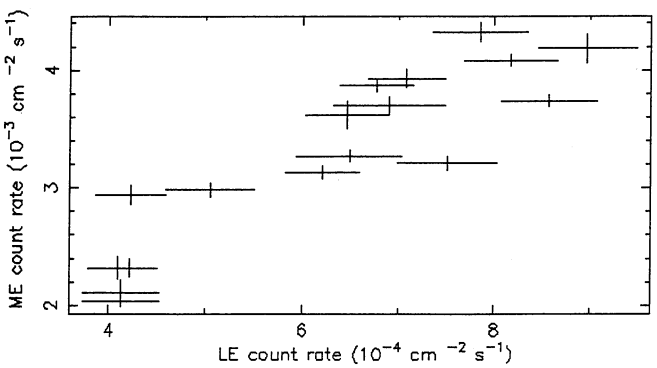

FIG. 11.—Observed count rates of LE vs. ME

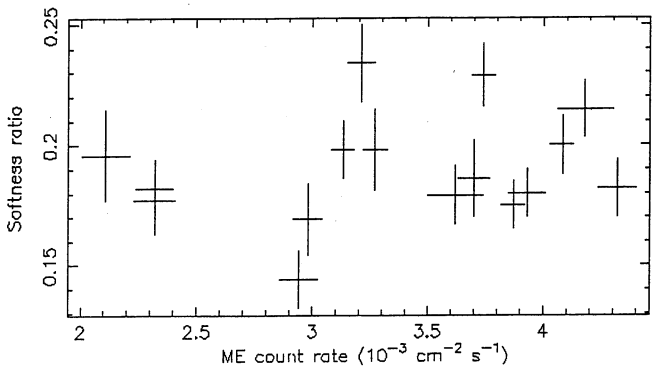

FIG. 13.—Same as Fig. 12, but for ME count rate. This figure shows that although the ME count rate and the softness varied, they are uncorrelated.

excess and the soft spectral slope were maximum and steepest, respectively, when this galaxy was in its brightest state (see Tables 1 and 4) and the hard spectral component was practically unchanged even though there were dramatic variations of the source. Since the basic mechanisms behind the origin and the variability of soft excess are yet largely unknown, at present, it is difficult to make any definite conclusion about it. However, here we will present one speculative scenario. On the basis of the present observations of 3C 382, we have suggested in § 3.1 that the soft and hard X-rays originate from distinct sources (most probably, the soft X-rays originate in an optically thin part of an accretion disk and the hard X-rays originate in an optically thick part of an accretion disk). Also, we have already seen that the soft excess was maximum when the source was brightest.

In a previous paper (Ghosh et al. 1991) we have discussed in detail that the variations of the X-ray luminosity of an AGN depend on the variations of the central continuum source. Again the continuum source can vary if there are variations of the accretion rate which depends on many parameters; one such important parameter is the distribution of matter, around the central compact object, to be accreted. Thus an AGN will be in a brighter state when the accretion rate is relatively higher. During the brighter state of the source, both the soft and hard X-ray fluxes will increase (as has been seen in 3C 382). If part of the hard X-rays which originate in an inner part (optically thick) of an accretion disk get reprocessed and emit soft X-rays (as it travels toward the outer part of the disk), then the source will become relatively softer. Also, the soft excess will be relatively stronger. This is what we have seen in 3C 382 during its brightest state (see Figs 6 and 7). Although the present scenario which is a purely speculative one matches with the observations of 3C 382, this must be considered to be tentative.

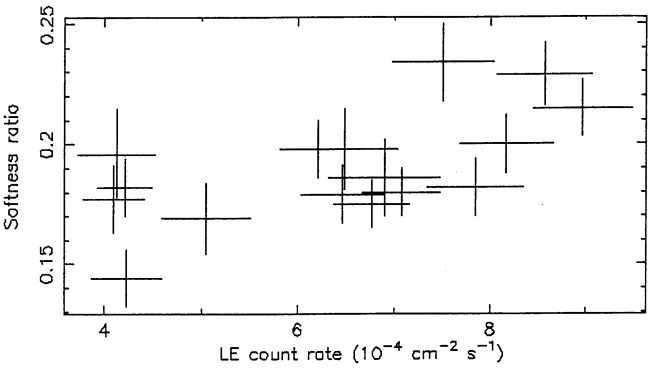

FIG. 12.—Plot of the LE count rate vs. the softness ratio which shows the correlated variability.

3.3. *Iron Line*

The measured line center energy of the Gaussian emission feature in the X-ray spectra of 3C 382 is 6.2 ± 0.6 keV (average value). This value of the line center energy is consistent with both fluorescence from thick cold iron K-line (at 6.4 keV) and helium-like iron line from highly ionized matter (near 6.7 keV). Also, the measured equivalent width of the iron line which ranges between 100 and 1100 eV, is also consistent with both cold and hotter material (6.4–6.7 keV).

Fe line flux and equivalent width are plotted against ME count rate in Figure 14. From this figure, it is evident that both the line flux and the equivalent width stayed roughly constant during *EXOSAT* observations. Also the *EXOSAT* observations of this galaxy show that the doubling time scale of the continuum flux variability was around 3 days (Barr & Mushotzky 1986). Thus this time scale of continuum flux variability and the lack of variations in equivalent width of the emission line suggest that the gas emitting the iron line lies no further than a few light-days from the central continuum source.

Recently Kastra et al. (1991) have detected an iron line in the spectra of 3C 382 from *Ginga* data. They have interpreted this

TABLE 4

MEASURED SOFT EXCESS IN 3C 382

Date (year/day)	Soft Excess[a]
1983/255	3.70 ± 0.80
1985/116	5.60 ± 1.60
1985/117	6.35 ± 1.60
1985/147	6.00 ± 2.00
1985/153	10.00 ± 2.30
1985/161	10.20 ± 2.30
1985/171	9.00 ± 1.50
1985/195	10.00 ± 1.80
1985/211	10.70 ± 1.50
1985/223	14.40 ± 2.20
1985/233	10.40 ± 1.50
1985/246	13.50 ± 2.00
1985/256	16.80 ± 2.00

[a] In units of 10^{-5} counts cm^{-2} s^{-1} keV^{-1}.

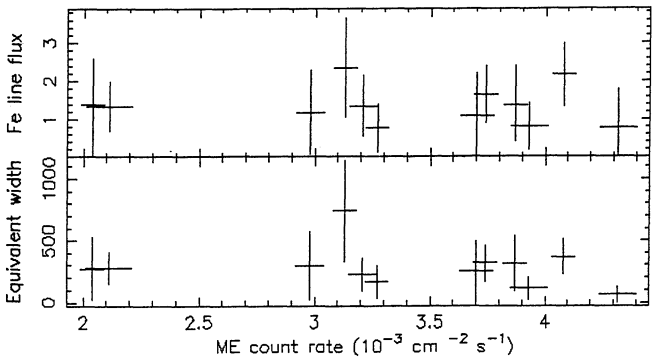

FIG. 14.—ME count rate is plotted against the Fe line flux (*upper panel*) and the equivalent width of the Fe line (*lower panel*). Both the Fe line flux and the equivalent width were roughly constant.

line as due to fluorescence in dense material around the central compact object. They have also suggested that the large equivalent width of this line (280 eV) may be either due to the large inclination of the accretion disk in this galaxy or due to time delay effects. We also suggest that the emission line detected at 6.2 ± 0.6 keV in the *EXOSAT* spectra of 3C 382 may be due to fluorescence of cold iron which lies close to the central continuum source ($\sim$ a few light-days from the continuum source).

4. CONCLUSIONS

Results of the spectral analysis of the X-ray spectra of 3C 382, obtained from *EXOSAT* observations, suggest the following results.

This galaxy was observed with *Ariel V* (Elvis et al. 1978), *HEAO 1* (Marshall et al. 1979; Dower et al. 1980), *Einstein* (Petre et al. 1984; Urry et al. 1989), *EXOSAT* (this work), and *Ginga* (Kastra et al. 1991) X-ray satellites between 1975 and 1989. The hard X-ray luminosity light curve constituted from the above observations shows a major outburst of this galaxy in 1985 during *EXOSAT* observations (see Fig. 5 of Kastra et al. 1991). Remarkable variations in the LE and ME bands (maximum to minimum variations were $\sim$120% and $\sim$110% in the LE and ME bands, respectively, with different rise/decay time scales) were observed in 3C 382 during the outburst. A prominent dip about halfway through is present in both the LE and ME light curves during the flare of this galaxy (see Fig. 1). Correlated variability was found only between the LE count rate and the softness ratio of this source (see Fig. 12), but the ME count rate which varied in correlation with the LE count rate has shown uncorrelated variability with the softness ratio. Also, the ME spectral slope was roughly constant ($\Gamma \sim 1.7 \pm 0.1$) during the *EXOSAT* observations (see Figs. 2 and 3). However, the LE spectral slope has displayed correlated variability with the LE count rate, with the soft excess, and with the softness ratio (see Fig. 9).

Variable soft excess detected in this galaxy is best fitted with the broken power law model (model 7) which suggests a variable soft spectral component below 0.6 keV and a nonvariable hard component between 0.6 and 10 keV.

We have detected an emission line at 6.2 ± 0.6 keV (average value) in the X-ray spectra of 3C 382. The measured equivalent width of this line ranges between 100 and 1100 eV. Also the line flux and the equivalent width of this line were almost constant during the flare (see Fig. 14). It has been suggested that the detected emission line may be due to fluorescence of cold iron around the central compact object and the cold gas emitting the iron line lies close (a few light-days) to the continuum source. Thus the X-ray spectrum (0.1–10 keV) of 3C 382 consists of three components: a variable soft spectral component below 0.6 keV, a nonvariable hard spectral component above 0.6 keV (0.6–10 keV), and an iron emission line around 6 keV.

We are grateful to Professor J. C. Bhattacharyya for his support and encouragement, in all respects. Our thanks to the *EXOSAT Observatory* staff, especially to N. E. White. A. N. Parmer, F. Habrel, P. Giommi, P. Barr, and A. M. T. Pollock, at ESTEC who helped us to get the data from the archives and provided us with the XSPEC software package. One of us, K. K. G., wants to express his sincere thanks to the *EXOSAT* staff for their help in data analysis during his stay at ESTEC. Our sincere thanks to the referee for valuable comments and suggestions.

REFERENCES

Barr, P., & Mushotzky, R. F. 1986, Nature, 320, 421
Burch, S. F. 1979, MNRAS, 186, 519
Czerny, B., & Elvis, M. 1987, ApJ, 321, 305
de Korte, P. A. J., Bleeker, J. A. M., den Boggende, A. J. F., Branduardi-Raymont, G., Culhane, J. L., Gronenschild, E. H. B. M., Mason, I., & McKechnie, S. P. 1981, Space Sci. Rev., 30, 495
Dower, R. G., Griffiths, R. E., Bradt, H. V., Doxsey, R. E., & Johnston, M. D. 1980, ApJ, 235, 355
Elvis, M., Maccacaro, T., Wilson, A. S., Ward, M. J., Penston, M. V., Fosbury, R. A. E., & Perola, G. C. 1978, MNRAS, 183, 129
Ghosh, K. K., & Soundararajaperumal, S. 1991, ApJ, 383, 574
Ghosh, K. K. Soundararajaperumal, S., Kalai Selvi, M., & Sivarani, T. 1991, A&A, in press
Kastra, J. S., Kunieda, H., & Awaki, H. 1991, A&A, 242, 27
Kruper, J. S., Urry, C. M., & Canizares, C. R. 1990, ApJS, 74, 347
Kunieda, H., Turner, T. J., Awaui, H., Koyama, K., Mushotzky, R., & Tsusaka, Y. 1990, Nature, 345, 786
Lampton, M., Margon, B., & Bower, S. 1976, ApJ, 208, 177
Lawrence, A., Watson, M. G., Pounds, K. A., & Elvis, M. 1985, MNRAS, 217, 685
Leighly, K. M., Pounds, K. A., & Turner, T. J. 1989, in Proc. 23rd ESLAB Symposium on Two Topics in X-Ray Astronomy (ESA SP-296), ed. J. Hunt & B. Battrick (Noordwijk: ESA), 961
MacDonald, G. H., Kenderdine, S., & Neville, A. C. 1968, MNRAS, 138, 259
Marshall, F. E., Boldt, E. A., Holt, S. S., Mushotzky, R. F., Pravdo, S. H., Rothschild, R. E., & Serlemitsos, P. J. 1979, ApJS, 40, 657
Morrison, R., & McCammon, D. 1983, ApJ, 270, 119
Mushotzky, R. F. 1984, Adv. Space. Res., 3, 157
Nandra, K., Pounds, K. A., Fabian, A. C., & Rees, M. J. 1989, MNRAS, 236, 39P
O'Dell, S. L., Puschell, J. J., Stein, W. A., Warner, J. W., & Ulrich, M.-H. 1978, ApJ, 219, 818
Osterbrock, D. E., Koski, A. T., & Phillips, M. M. 1975, ApJ, 197, L41
———. 1976, ApJ, 206, 898
Parma, P., de Ruiter, H. R., Fanti, C., & Fanti, R. 1986, A&AS, 64, 135
Petre, R., Mushotzky, R. F., Krolik, J. H., & Holt, S. S. 1984, ApJ, 280, 499
Pounds, K. A., Nandra, K., Stewart, G. C., George, I. M., & Fabian, A. C. 1990, Nature, 344, 132
Pounds, K. A., Nandra, K., Stewart, G. C., & Leighly, K. 1989, MNRAS, 240, 769
Preuss, E., & Fosbury, R. A. E. 1983, MNRAS, 204, 783
Puschell, J. J. 1981, AJ, 86, 16
Reichert, G. A., Wu, C.-C., Bogess, A., & Oke, J. B. 1985, BAAS, 17, 578
Riley, J. M., & Branson, N. J. B. A. 1973, MNRAS, 164, 271
Singh, K. P., Rao, A. R., & Vahia, M. N. 1990, MNRAS, 246, 706
Stark, A. A., Heiles, C., Bally, J., & Linke, R. 1992, in preparation
Storm, R. G., Willis, A. G., & Wilson, A. S. 1978, A&A, 68, 367
Tadhunter, C. N., Perez, E., & Fosbury, R. A. E. 1986, MNRAS, 219, 555
Turner, M. J. L. T., Smith, A., & Zimmermann, H. U. 1981, Space Sci. Rev., 30, 513
Turner, T. J., & Pounds, K. A. 1989, MNRAS, 240, 833
Urry, C. M., Arnaud, K., Edelson, R. A., Kruper, J. S., & Mushotzky, R. F. 1989, in Proc. 23rd ESLAB Symposium on Two Topics in X-Ray Astronomy (ESA SP-296), ed. J. Hunt & B. Battrick (Noordwijk: ESA), 789
White, N. E., & Peacock, A. 1988, Mem. Soc. Astron. Ital., 59, 7
Wilkes, B. J., & Elvis, M. 1987, ApJ, 323, 243
Wilkes, B. J., Masnov, J.-L., Elvis, M., McDowell, J., & Arnaud, K. 1989, in Proc. 23rd ESLAB Symposium on Two Topics in X-Ray Astronomy (ESPA SP-296), ed. J. Hunt & B. Battrick (Noordwijk: ESA), 1081
Yee, H. K. C., & Oke, J. B. 1978, ApJ, 226, 753
———. 1981, ApJ, 248, 472